# Short Papers

## A Microwave Measurement Technique for Characterizing the I–V Relationship for Negative Differential Conductance Devices

P. Huang, D. S. Pan, N. C. Luhmann, Jr.

*Abstract*—**The practical procedures of a recently proposed technique to experimentally determine the I–V characteristics of negative differential conductance (NDC) devices are presented in this paper. The technique employs microwave reflection coefficients together with the measurable portions of the device's I–V characteristics to infer the I–V curve in the negative conductance region where oscillations tend to occur under normal dc bias conditions. The effects of higher harmonics at large signal levels are also taken into account in the calculation. The advantages of the method for high NDC devices have been pointed out in the stability analysis contained in a previously published letter [17]. The technique was demonstrated in the case of a low NDC tunnel diode where the agreement between the deduced I–V curve using the described method and the dc measured I–V curve is within 5%. The I–V curve in the negative conductance region for another tunnel diode with much higher negative conductance is also obtained and a self-consistent accuracy of 5% is found.**

### I. Introduction

Since the discovery of the tunneling phenomenon in narrow germanium $p$-$n$ junctions by $L$. In [1], negative differential conductance (NDC) tunneling devices such as tunnel diodes and, more recently, quantum well diodes have stimulated significant research activity. Interest in these structures is due to their potential for generating power as oscillators [2]–[4], as well as serving as frequency multipliers [5] together with their capability of providing high frequency response [6], both of which make NDC devices ideal candidates for millimeter and submillimeter wave sources. Also, with today's refined device fabrication technology, the use of double-barrier quantum well structures in the terahertz region has become realizable due to the continuing decrease in the barrier width [7], resulting in the practicality of currently available resonant tunneling structures for high frequency devices.

The successful fabrication of quantum well diodes that exhibit negative conductance at room temperature has been reported by numerous groups [6], [8]–[10]. Unfortunately, all of the measured I–V characteristics reported have exhibited significant oscillation in the NDC region [11]–[14]. The existence of RF oscillations tends to hinder the dc I–V curve measurement under normal conditions. This is a particular problem for devices with large negative conductance since it is extremely difficult to eliminate the oscillations. This is unfortunate because the detailed shape of the I–V curve, particularly the portion in the NDC regime, provides important information for device modeling and circuit design.

Significant effort has been devoted to solving this problem by a number of researchers. For example, Chua *et al.* have constructed a negative resistance I–V curve tracer that measures the I–V characteristics of two-terminal and three-terminal nonlinear devices [15]. Shewchuk *et al.* have reported another technique to suppress the device oscillations by using a microwave circuit with ac loading [16]. Recently, we have investigated a new approach to recover the I–V characteristics of NDC devices employing microwave reflection coefficients. A preliminary account of this work has been published in a letter [17]. In that letter, the principles of the new technique were addressed, but the practical details of the technique were not covered due to space limitations. In this current paper, we provide a more detailed presentation of the procedures of the technique. In the next section, the experimental setup as well as the analytical procedure will be described in detail. The results from a proof-of-principle experiment will be presented in Section III. For the principles and theoretical background, we refer the readers to our previous publication [17].

Manuscript received August 24, 1992; revised January 14, 1993. This work was supported by TRW under the California MICRO program and by the UCLA Joint Services Electronics Program

The authors are with the Department of Electrical Engineering, University of California, Los Angeles, Los Angeles, CA 90024.

IEEE Log Number 9210218.

### II. Experimental Approach and Analysis

As stated in our previous letter [17], dc biasing a negative conductance device such as a tunnel diode in its NDC region always presents difficulty. To remedy this, the diode can be biased in its positive differential conductance (PDC) region and be driven into its NDC region by appropriate RF signal levels. This not only ensures a stable biasing point. the use of the PDC region also helps in stabilizing the measurement circuitry. A stability analysis has been included in the previously published letter [17]. From that analysis, it is clear that the biasing and measurement circuitry for the $S$-parameter measurement approach have more flexibility than that of using a curve tracer. This advantage can be seen in the work reported by Owen *et al.* [18]. The instability in $S$-parameter measurements can therefore be minimized when the dc bias is set in the PDC region. Furthermore, large signal analysis of two-terminal devices is a well developed technique [19]. Therefore, we can accurately measure the NDC region of the dc I–V characteristics of NDC devices by utilizing the large signal $S$-parameter information. The procedures are outlined in the following.

Since the diode bias point is chosen to lie in the PDC region, large RF signal levels must eventually be applied in order to cover the NDC region. As a result, higher harmonics must be self-consistently treated to ensure sufficient measurement accuracy. An appropriate analysis program has been developed by Siegel *et al.* [19] based on the large signal analysis technique devised by Kerr [20]. Starting with a stable dc bias point as shown in Fig. 1, for example, and the stable portion of the I–V characteristics, by increasing the RF voltages in small increments and measuring the corresponding $S$-parameters, we can map out the I–V characteristics in the NDC region through the analysis depicted in Fig. 1. Fig. 1 illustrates the procedure to recover the I–V curve in the NDC region segment by segment. If the diode is biased at a value of $V_{\mathrm{dbias}}$ near the valley voltage, $V_{\mathrm{v}}$, and a small RF signal $V_{\mathrm{RF}}(1)$ is applied across the diode, a linear segment extending approximately from ($V_{\mathrm{dbias}}$-$V_{\mathrm{RF}}(1)$) to $V_{\mathrm{dbias}}$ is needed to approximate the I–V curve. Applying a second RF signal $V_{\mathrm{RF}}(2)$ that is slightly greater than $V_{\mathrm{RF}}(1)$ would require a second linear segment approximately from ($V_{\mathrm{dbias}}$-$V_{\mathrm{RF}}(2)$) to ($V_{\mathrm{dbias}}$-$V_{\mathrm{RF}}(1)$). Continually applying larger RF signal levels and adjusting the slopes of the approximating linear segment each time to match the calculated conductance to the measured value would then result in the I–V curve in the NDC region. Similarly, if the diode is

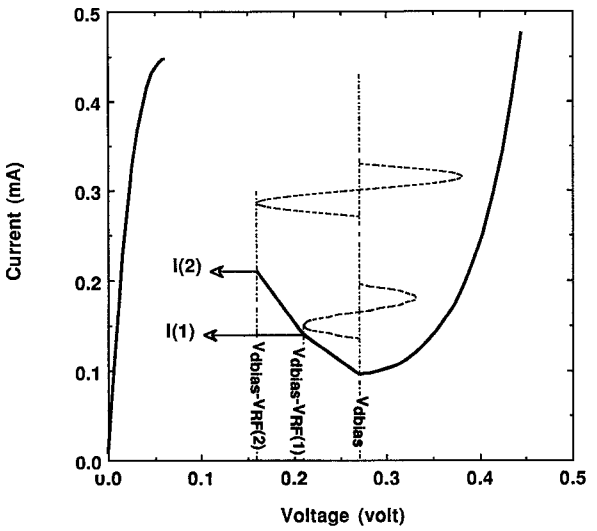


Fig. 1. The procedure to calculate the I–V curve with the diode biased near the valley voltage.

biased at a value near the peak voltage, $V_p$, the I–V curve can be piece-wisely reconstructed from $V_p$ into the NDC region.

To carry out his procedure, we need to measure $V_{\rm RF}$ and $S$-parameters accurately. Modern network analyzers have very high measurement precision at variable power levels and frequencies. Each RF power level can be monitored with a power meter placed at the input of the test fixture. However, since the described technique starts with very small RF signal levels, the accuracy of the measured RF power levels may not be as good at small RF signal levels. Therefore, to precisely determine $V_{\rm RF}$, we found that it is most convenient to measure the "rectified" dc bias current instead of measuring the input RF power levels. This is because the current meter has much higher precision than the power meter, especially when the RF signal levels are small. In addition, the rectified current can be accurately calculated by the large signal analysis program [19].

The embedding circuit must be predetermined up to a sufficient number of harmonics (six in our case). The device parameters $R_s$, $L_s$ and $C$ (junction capacitance) can be determined experimentally. The information concerning I–V characteristics is contained in $G$ (the intrinsic negative conductance) The device tested is voltage biased at $V_{\rm dbias}$. For the $n^{\rm th}$ RF input power level, the $S$-parameter and dc rectified current are measured. Since only an incremental portion of the I–V curve in the NDC region needs to be determined, it requires two variables , namely $V_{\rm RF}(n)$ and $I(n) = I(V_{\rm dbias} - V_{\rm RF}(n))$ (see Fig. 1) to determine the segment. In the analysis, we determine $V_{\rm RF^{in}}(n)$ and $I(n)$ by adjusting them until the program generates $S_{11}$ and dc rectified current values that are in agreement with the measured values within a preset tolerance. Note that $V_{\rm RF}(n)$ is the RF voltage at the terminals of the device. We found that it is easier to first fit the dc rectified current with $V_{\rm RF}(n)$, then adjust $I(n)$ to fit $S_{11}$. To obtain good agreement for both current and $S_{11}$, $V_{\rm RF}(n)$ and $I(n)$ must be adjusted iteratively. The calculated $V_{\rm RF}(n)$ and $I(n)$ can thus be used in determining the I–V characteristics.

For a diode with low negative conductance, it is possible to bias the diode quite near $V_v$ or $V_p$ and still obtain a stable bias and $S_{11}$ measurement. This permits one to fully utilize the PDC portion of the I–V curve. However, if the $S$-parameters of a highly negative conductance diode are to be measured, the PDC region sometimes can not provide sufficient stabilization when the device is driven far into the NDC region by large RF signal levels. In this case, the diode needs to be biased further in the PDC region to utilize more of the PDC region for stabilization. Consequently, large RF signal levels are needed in order to cover the entire NDC region. An alternative way is to calculate the I–V characteristics using more than one bias point. For instance, the diode can be biased near $V_p$ and be driven by RF signal levels into the mid NDC region. Thus, half of the I–V curve in the NDC region can be deduced from the $S_{11}$ measurement with a dc bias near $V_p$. The remaining portion of the NDC region can be characterized by a second $S_{11}$ measurement with the diode biased near $V_v$. For devices with low NDC, $S_{11}$ can be also measured at $V_{\rm dbias}$ near $V_v$ and $V_p$. The I–V curves thus constructed from both sets of $S_{11}$ measurements can be overlapped for better accuracy and confidence.

## III. Results

Several proof-of-principle experiments have been performed on commercially available tunnel diodes in the course of this work to verify the validity of the above mentioned technique. Each diode was mounted on a test fixture with a 50-Ω transmission line. The measuring circuit consists of a 50-Ω load from the network analyzer signal source connected to a directional coupler with the output port of the coupler connected to an HP11590A Bias Network and the test fixture with the device. The power meter monitors the RF power incident on the device and the current meter monitors the dc current (bias and "rectified" current) at each power level. Calibration was carried out with a short and a 50-Ω load at the position of the tunnel diode as well as an open end transmission line. Hence, the measuring circuit presents a 50-Ω impedance to the device. The value of $S_{11}$ for the device was measured at 150 MHz to ensure the existence of the device negative conductance. Moreover, at such a low frequency, the effects of the reactive elements of the device are not very significant.

The first tunnel diode that was tested has relatively low negative conductance. The peak and valley points are located at 0.061 V and 0.268 V, respectively. The peak current is approximately 0.45 mA and the valley current is about 0.085 mA. By placing a 340-Ω resistor in parallel with the diode, we were able to directly measure the entire dc I–V curve using a standard parameter analyzer. This is shown as the solid curve in Fig. 2. $S_{11}$ of the device was measured with the device first biased at 0.0543 V. The circles shown in Fig. 2 represent the I–V points deduced from this $S_{11}$ measurement. A second $S_{11}$ measurement was made with the diode biased at 0.2806 V. The de-embedded I–V curve is shown as the squares in Fig. 2. As can be seen from Fig. 2, both sets of $S_{11}$ measurements generated I–V characteristics in the NDC region that are in good agreement with the directly measured I–V curve of the device. For both cases, the deviation is within 5% of the measured I–V curve.

A second tunnel diode with high negative conductance was also tested. This diode has peak current of 4.75 mA at 0.07 V and a valley current of 0.36 mA at 0.37 V. To fully recover the I–V curve in the NDC region, we had to utilize $S_{11}$ measurements taken at 0.0349 V and 0.295 V as was discussed in the previous section. The I–V characteristics thus obtained have been reported in the paper published earlier [17]. Since we were unable to measure the entire dc I–V curve directly due to the device's higher negative conductance, a direct comparison between the measured and deduced I–V curves is not available. However, it should be noted that the two halves of the deduced I–V curve do converge to within 5% of each other in the NDC region, lending further confidence to the viability of the technique.

It is interesting to note that any fine structure in the NDC region can be reflected in the $S_{11}$ measurement. To confirm the possibility of measuring such structure, we have generated an I–V curve with "artificial" local maxima in the NDC region. Instead of being

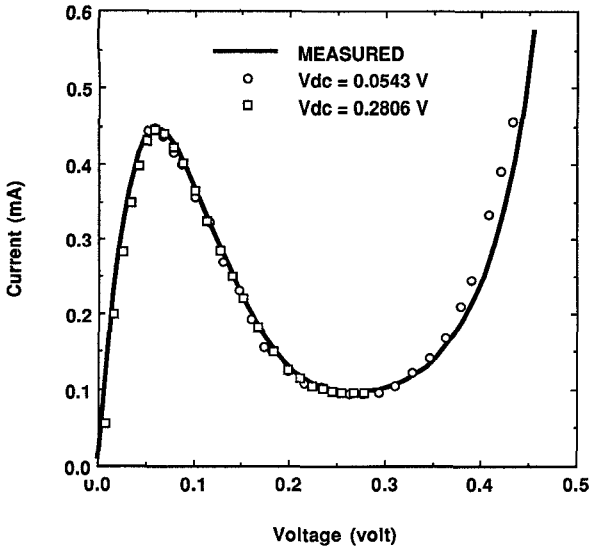


Fig. 2 De-embedded and dc measured I–V curves of a tunnel diode with low negative differential conductance.

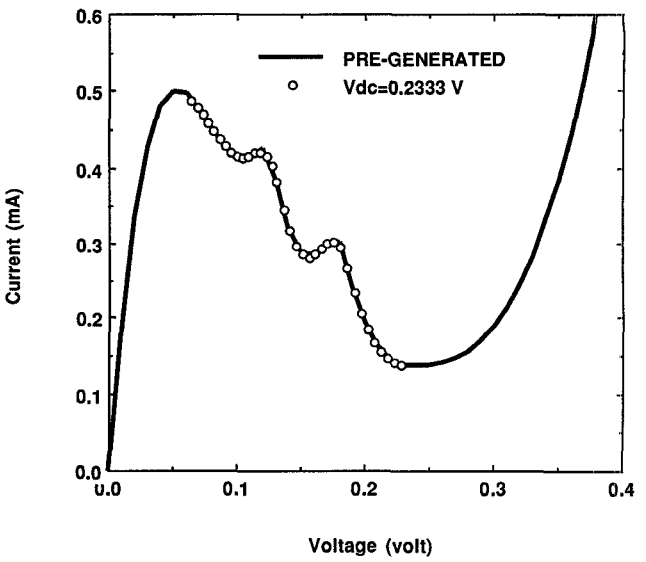


Fig. 3. De-embedded and pre-generated artificial I–V characteristics. The solid line is an artificial I–V curve with fine structure in the negative resistance region. The circles are generated numerically according to the procedure of this work.

measured experimentally, the values of $S_{11}$ and the dc rectified current were calculated using this I–V curve and an appropriate dc bias point. Using the I–V curve in the PDC region together with the calculated values of $S_{11}$ and rectified current, we were able to reconstruct the I–V curve in the NDC region which also shows the same local maxima. The results are illustrated in Fig. 3 where the solid curve is the pre-generated I–V curve and the circles were deduced from the $S_{11}$ of this "imaginary" device. This reconstruction of the I–V curve shows the numerical soundness of our procedure even for the more complicated NDC region. Currently, to our knowledge, there are no experimental data which show this fine structure. Part of the reason is that most of the NDC regions of devices such as resonant tunneling diodes are usually not measured. For resonant tunneling diodes with more than one quasi-bound state in the quantum well, such fine structure can be expected. This situation may occur in $n$-type resonant tunneling diodes with a recessed quantum well. It may also happen in p-type resonant tunneling diodes due to the degeneracy of the bulk valence band edge.

## IV. Conclusion

In conclusion, we have described a novel method to recover the I–V characteristics in the NDC region of nonlinear devices. This method was first tested against a tunnel diode whose negative conductance is sufficiently low such that its complete I–V curve can be measured using conventional techniques. The accuracy between the deduced (using the described approach) and measured I–V curves is shown to be within 5%. The I–V curve in the NDC region of another tunnel diode with much higher negative conductance has also been determined. Although we were unable to compare the deduced I–V curve with the dc measured I–V for the second diode, a convergence of the two halves of the I–V curve in the NDC region was obtained. Finally we were also successful in reconstructing an artificially generated I–V curve with local maxima in the NDC region based on the $S_{11}$ and the rectified current calculated from the I–V characteristics. Together with other methods that have been developed to measure the I–V charcteristics of nonlinear devices, this method can serve as a tool to assist in circuit design and device modeling

## Acknowledgment

The authors wish to thank P. McDonald and M. Espiau for their expert technical assistance and J. M. Gering of University of Illinois at Urbana-Champaign for providing us with a thesis and publications from his group.

## References

[1] L. Esaki, "New phenomenon in narrow germanium $p$-$n$ junctions," *Phys. Rev.*, vol. 109, pp. 603–604, 1958.

[2] E. R. Brown, T. C. L. G. Sollner, W. D. Godhue, and C. D. Parker, "Millimeter-band oscillations based on resonant tunneling in a double-barrier diode at room temperature," *Appl. Phys. Lett.*, vol. 50, pp. 83–85, Jan. 1987.

[3] T. C. L. G. Sollner, P. E. Tanenwald, D. D. Peck, and W. D. Goodhue, "Quantum well oscillators," *Appl. Phys. Lett.*, vol. 45, p. 1319, 1984.

[4] E. R. Brown, J. R. Soderstrom, C. D. Parker, L. J. Mahoney, K. M. Molvar, and T. C. McGill, "Oscillations up to 712 GHz in InAs/AlSb resonant-tunneling diodes," *Appl. Phys. Lett.*, vol. 53, pp. 2291–2293, May 1991.

[5] P. D. Batelaan and M. A. Frerking, "Quantum well multipliers," presented at the 12th International Conference on Infrared and Millimeter Waves, Lake Buena Vista, Fl., 1987.

[6] T. C. L. G. Sollner, W. D. Goodhue, P. E. Tannenwald, C. D. Parker, and D. D. Peck, "Resonant tunneling through quantum wells at frequencies up to 2.5 THz," *Appl. Phys. Lett.*, vol. 43, pp. 588–590, Sept. 1983.

[7] D. S. Pan and C. C. Meng, "On the mechanism and frequency limit of double-barrier quantum-well," *J. Appl. Phys.*, vol. 61, pp. 2082–2084, Mar. 1987.

[8] H. Toyoshima, Y. Ando, A. Okamoto, and T. Itoh, "New resonant tunneling diode with deep quantum-well," *Jpn. J. Appl. Phys.*, vol. 25, pp. 786–788, Sept. 1986.

[9] G. S. Lee, K. Y. Hsieh, and R. M. Kolbas, "Room-temperatures negative differential resistance in strained-layer GaAs-AlGaAs-InGaAs quantum well heterostructures," *Appl. Phys. Lett.*, vol. 49, pp. 1528–1530, Dec. 1986.

[10] T. Inata, S. Muto, Y. Nakata, S. Sasa, T. Fuji, and S. Hiyamizu, "A pseudomorphic $In_{0.53}Ga_{0.47}As/AlAs$ resonant tunneling barrier with a peak-to-valley ratio of 14 at room temperature," *Jpn. J. Appl. Phys.*, vol. 26, pp. 1332–1334, Aug. 1987.

[11] V. P. Kesan, A. Mortazawi, D. R. Miller, V. K. Reddy, D. P. Neikirk, and T. Itoh, "Microwave and millimeter-wave QWITT diode oscillators," *IEEE Trans. Microwave Theory Tech.*, vol. MTT-37, no. 12, pp. 1933–1940, Dec. 1989.

[12] J. R. Soderstrom, D. H. Chow, and T. C. McGill, "InAs/AlSb double-barrier structure with large peak-to-valley current ratio: a candidate for high frequency microwave devices," *IEEE Electron Device Lett.*, vol. EDL-11, no. 1, pp. 27–29, Jan. 1990.
[13] T. P. E. Broekaert and C. G. Fonstad, "Extremely high current density, low peak voltage, pseudomorphic $In_{0.53}Ga_{0.47}As/AlAs/InAs$ resonant tunneling diodes," *Proc. Int. Electron Devices Meet.*, vol. IEDM-89, pp. 559–562, 1989.
[14] B. G. Park, E. Wolak, K. L. Lear, and J. S. Harris, Jr., "Improved vertically integrated resonant tunneling diodes," *Proc. Int. Electron Devices Meet.*, vol. IEDM-89, pp. 563–566, 1989.
[15] L. O. Chua and G. Q. Zhong, "Negative resistance curve tracer," *IEEE Trans. Circuits Syst.*, vol. CAS-32, pp. 569–582, June 1985.
[16] T. J. Shewchuk, J. M. Gering, P. C. Chapin, P. D. Coleman, W. Kopp, C. K. Peng and H. Morkoc, "Stable and unstable current-voltage measurements of a resonant tunneling heterostructure oscillator," *Appl. Phys. Lett.*, vol. 47, pp. 986–988, Nov. 1985.
[17] P. Huang, D. S. Pan, and N. C. Luhmann, Jr., "A new method of determination of the I–V characterisitics of negative differential conductance devices by microwave reflection coefficient measurements," *IEEE Electron Device Lett.*, vol. EDL-11, pp. 570–572, Dec. 1990.
[18] M. Owens, D. J. Halchin, K. L. Lear, W. S. Lee, and J. S. Harris, Jr., "Microwave characteristics of MBE grown resonant tunneling devices," *1989 IEEE MTT-S Int. Microwave Symp. Dig.*, pp. 471–474, 1989.
[19] P. Siegel, A. R. Kerr, and W. Hwang, "Topics in the optimization of millimeter wave mixers," NASA Tech. Paper 2287, 1984.
[20] A. R. Kerr, "A technique for determining the local oscillator waveforms in a microwave mixer," *IEEE Trans. Microwave Theory Tech.*, vol. MTT-23, no. 10, pp. 828–831, Oct. 1975.

# Scattering and Reception by a Flanged Parallel-Plate Waveguide: TE-Mode Analysis

Tah J. Park and Hyo J. Eom

***Abstract*—The TE-mode characteristics of scattering and reception by a flanged parallel-plate waveguide are examined. The Fourier transform is used to represent the scattered fields in the spectral domain. The simultaneous equations for the transmitted field coefficients are solved to obtain the solution in an asymptotic series form. Numerical computations are performed to illustrate the behaviors of the scattered field and the transmission coefficients versus the aperture size.**

## I. Introduction

Electromagnetic scattering from a conducting double-wedge has been extensively studied with asymptotic high-frequency techniques [1], [2] since an exact closed-form solutionis still unknown. TM-mode scattering from a flanged parallel-plate waveguide (a special double-wedge geometry) was considered in [3] using the Weber–Schafheitlin integral technique. In this paper, we examine TE-mode scattering from the flanged waveguide by utilizing the Fourier transform and the mode-matching technique [4], [5]. In the next section, we present the scattered field as an asymptotic series which can be represented in closed form in high-frequency limit. Numerical computations are presented to illustrate the behaviors of the scattered field and the transmission coefficient. A brief summary of the theoretical development is given.

Manuscript received January 30, 1992; revised December 21, 1992.

The authors are with the Department of Electrical Engineering, Korea Advanced Institute of Science and Technology, 373-1, Kusong-dong, Yusong-gu, Taejon, Korea.

IEEE Log Number 9210207.

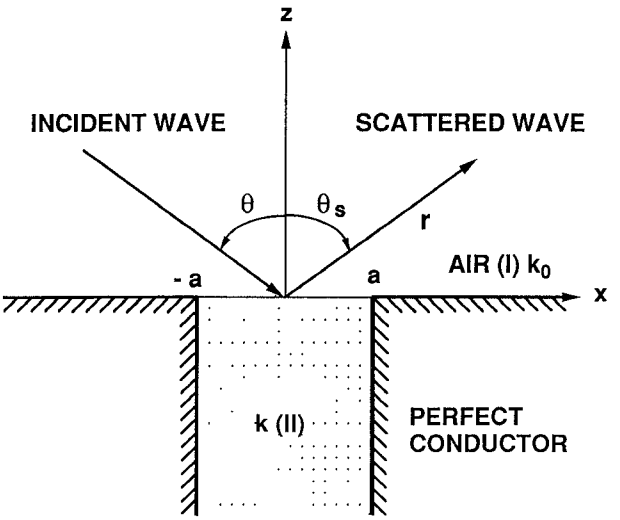


Fig. 1.

## II. Scattered and Received Fields Derivation

Fig. 1 shows a perfect-conducting, flanged, parallel-plate waveguide of width $2a$. In Region I ($z > 0$) an incident field $E_y^i$ (TE mode: transverse-electric-to-propagation-direction) impinges on the flanged parallel-plate waveguide. Region II ($z < 0$, $-a < x < a$) denotes the waveguide interior. The wave numbers of Regions I and II are $k_o (= 2\pi/\lambda)$ and $k$, respectively, and the time factor $e^{-j\omega t}$ is suppressed.

In Region I the total electric field consists of the incident, reflected, and scattered fields which are written as

$$E_y^i(x,z) = e^{jk_x x - jk_z z}$$
$$E_y^r(x,z) = -e^{jk_x x + jk_z z}$$
$$E_y^s(x,z) = 1/(2\pi)\int_{-\infty}^{\infty} \hat{E}_y^s(\zeta) e^{-j\zeta x + jk_1 z}\, d\zeta$$

where

$$k_x = k_0 \sin\theta$$
$$k_z = k_0 \cos\theta$$
$$k_1 = \sqrt{k_0^2 - \zeta^2}$$
$$\hat{E}_y^s(\zeta) = \int_{-\infty}^{\infty} E_y^s(x,0) e^{j\zeta x}\, dx\,.$$

Since $H_x(x,z) = -1/(j\omega\mu)\partial E_y(x,z)/\partial z$, the corresponding $x$ components of the incident, reflected, and scattered $H$ fields may be readily obtained.

In Region II the total transmitted field may be represented as

$$E_y^t(x,z) = \sum_{m=1}^{\infty} d_m \sin a_m(x+a) e^{-j\xi_m z} \qquad (1)$$

where

$$a_m = m\pi/(2a)$$
$$\xi_m = \sqrt{k^2 - a_m^2}\,.$$

To determine the unknown coefficients $d_m$ it is necessary to enforce continuity in the tangential $E$ and $H$ fields. First, continuity of the tangential $E$ field along the $x$–axis yields

$$E_y^s(x,0) = E_y^t(x,0) \quad |x| < a$$
$$= 0 \quad |x| > a\,.$$